Title: Mesoscale corticocortical connectivity corresponds with intracortical microstimulation-evoked neural activity

Authors: David T. Bundy[1], Scott Barbay[1], Heather M. Hudson[1], Shawn B. Frost[1], Randolph J. Nudo*[1,2], David J. Guggenmos[1]

Author Affiliations:

[1]Departiment of Rehabilitation Medicine, University of Kansas Medical Center, Kansas City, KS, USA

[2]Landon Center on Aging, University of Kansas Medical Center, Kansas City, KS, USA

*Corresponding Author: Randolph Nudo: rnudo@kumc.edu

Highlights

- Short-latency neural responses to single-pulse intra-cortical microstimulation (ICMS) was evaluated as a surrogate for anatomical connectivity.
- Across three new-world monkeys, the strength of neural responses strongly correlated with known anatomical connections.
- Neural responses to stimulation were repeatable across the duration of the experiments and were invariant to minor deviations in electrode positions and anesthetic state.

Abstract

Background: Cortical stimulation has been a versatile technique for examining the structure and function of cortical regions as well as for implementing novel therapies. While stimulation has been used to examine the local spread of neural activity, it may also enable longitudinal examination of mesoscale interregional connectivity. Recent studies have used focal intracortical microstimulation with optical imaging to show cross-region spread of neural activity, but the exact neural mechanisms elucidated by these modalities is uncertain. *Objective:* Here, we sought to use intracortical microstimulation (ICMS) in conjunction with recordings of multi-unit action potentials to assess the mesoscale effective connectivity within sensorimotor cortex. *Methods:* Neural recordings were made from multielectrode arrays placed into sensory, motor, and premotor regions during surgical experiments in three squirrel monkeys. During each recording, single-pulse ICMS was repeatably delivered to a single region. Mesoscale effective connectivity was calculated from ICMS-evoked changes in multi-unit firing. *Results:* Multi-unit action potentials were able to be detected on the order of 1 ms after each ICMS pulse. Across sensorimotor regions, short-latency (<2.5 ms) ICMS-evoked neural activity strongly correlated with known anatomic connections. Additionally, ICMS-evoked responses remained stable across the experimental period, in spite of small changes in electrode locations and anesthetic state. *Conclusions:* These results show that monitoring ICMS-evoked neural activity is a viable way to longitudinally assess effective connectivity, enabling studies comparing the time course of connectivity changes with the time course of changes in behavioral function.

Keywords: Intra-cortical microstimulation, effective connectivity, anatomical connectivity

Introduction

Electrical stimulation of the brain is a versatile clinical and scientific tool. Clinically, stimulation can be used to modify the excitability of cortical regions (1, 2), map functional brain regions prior to neurosurgical resections (3), and drive artificial input into sensory cortices (4, 5). In research settings, stimulation can also be driven through small electrodes implanted into the cortex in a technique known as intracortical microstimulation (ICMS). ICMS activates a more focal region of the brain and has helped elucidate the structure and function of brain regions. ICMS in awake, behaving animals can modulate behavior, showing the functional roles of brain regions (6). ICMS has also been used to examine changes in the organization of motor cortex following behavioral training and post-stroke recovery (7-11).

Because of the varied applications of cortical stimulation, studies have examined the direct and indirect impacts of stimulation on neural circuits. Stimulation directly activates neurons, with axons activated at lower currents than cell bodies (12-15). However, the specific neural components activated depend on the excitability of the neural component, the distance from the electrode, stimulus amplitude, and stimulus duration (14, 15). Even at low amplitudes, stimulation can evoke transsynaptic activity (16), which underlies the potential to use stimulation to examine corticocortical connectivity.

Traditionally, investigations into corticocortical connectivity have relied on examining the pattern of fiber degeneration following a lesion (17) or injection of anatomical tracers (18-21). These methods have revealed extensive interareal connectivity, but they are limited to injecting tracers into a few distinct regions at a single time point. Because changes in connectivity are associated with neural injuries and disorders, this lack of temporal resolution is a significant limitation in interpreting the role of structural reorganization in functional recovery.

An alternative to these anatomical approaches is to measure evoked neural activity following ICMS. Recently, this method has been used with intrinsic optical imaging and functional magnetic resonance imaging (fMRI) to demonstrate intra- and interregional connectivity (22-26). However, because these modalities measure the hemodynamic response, it is difficult to separate synaptic activity from neural firing and to isolate direct anatomical projections with short latency responses (26).

We propose a novel method to examine mesoscale corticocortical connectivity that uses direct recordings of multi-unit neural activity to measure ICMS-evoked neural activity. When combined with an algorithm to remove stimulus artifact, we were able to examine short-latency neural responses to electrical stimuli on the order of 1 ms after a stimulus pulse. Importantly, this allows us to identify direct connections by differentiating short-latency action potentials from either polysynaptic action potentials or sub-threshold synaptic potentials.

Methods

Experimental Design

We performed intraoperative recordings in 3 male squirrel monkeys (*Saimiri sciureus*). The squirrel monkey is a new world monkey with a relatively lissencephalic cortex, allowing visualization of sensorimotor regions on the surface of the brain. All procedures were approved by the Institutional Animal Care and Use Committee at the University of Kansas Medical Center in compliance with *The Guide for the Care and Use of Laboratory Animals* (27). At the conclusion of the described experiments, monkeys were utilized for a secondary study (28).

Motor Mapping

Details of the surgical procedures have been described previously (10). Following a craniectomy, motor and premotor cortices were mapped using ICMS under ketamine anesthesia.

A photograph of the exposed cortex was taken to derive a two-dimensional sensorimotor map. For motor mapping, a microelectrode was made from a glass micropipette tapered to a fine tip and filled with 3.5M NaCl and inserted into cortex to a depth of 1750 μm (Layer 5). Pseudo-biphasic stimulus pulses were delivered as described previously (cathode leading, 200 μs/phase, 13 pulse train at 350 Hz, repeated once per second) (10). Stimulation current was increased slowly until a visible movement was elicited on at least 50% of stimuli or a maximum current of 30 μA was reached with no response observed. Upper limb movements were classified as either digit, distal forelimb, or proximal forelimb. Electrode penetrations were made at a spatial resolution of ~500 μm with finer resolution used as needed to delineate the borders between regions. The M1, PMv, and PMd distal forelimb regions were identified by defining boundaries between areas at which stimulation evoked digit, wrist, or forelimb movements and sites with more proximal elbow, shoulder, trunk or face movements. In addition to the distal forelimb regions, in two monkeys, a face region was identified rostral to the M1-DFL between the PMv and PMd distal forelimb regions.

Sensory Mapping

To determine boundaries between somatosensory regions (areas 3a, 3b, 1, and 2/5) a single-shank 16-contact linear multi-electrode array (Neuronexus, Ann Arbor, MI) was inserted into cortex to record multi-unit activity within a cortical column up to a depth of 1500 μm. Signals were filtered, amplified, and played on a speaker to monitor modulation in multi-unit firing. Cutaneous receptive fields were defined using Semmes-Weinstein monofilaments, and deep receptive fields were determined using high-threshold manual stimulation and joint manipulation. Area 3a was characterized by sites with multi-digit cutaneous receptive fields, and areas 3b and 1 were characterized by small cutaneous receptive fields that mirrored each other

with distal to proximal hand sites arranged in a rostral to caudal orientation in area 3b and a caudal to rostral orientation in area 1 (29). Caudal to area 1, sites had multi-digit receptive fields sensitive to proprioceptive stimuli. As the presence of area 2 in squirrel monkeys is uncertain (30, 31), sites caudal to area 1 were classified as area 2/5.

Neural Recordings

After cortical mapping, neural activity was recorded from multiple regions during single-pulse ICMS. All recordings and stimulation were made with an Intan RHS Stim/Record system (Intan Technologies, Los Angeles, CA). Three 32-channel electrode arrays (4 shanks x 8 sites per shank, 703 μm^2 site area, 100 μm site spacing, 400 μm shank spacing) were used.. One electrode array was placed in S1 (targeting areas 3a, 3b, 1, 2/5), a second array was placed in M1-DFL, and a final array was placed in premotor cortex (targeting PMv-DFL, PMd-DFL, and PM-face). Electrodes were inserted to depths of 1750 μm (M1 and PM) and 1500 μm (S1). Area 2/5 was only exposed in monkey 2, and the PM-face region was not recorded from in monkey 3. In monkey 1 the S1 and M1 electrode arrays each had four sites activated to reduce the electrode impedance and allow for both stimulation and recording. In monkeys 2 and 3, all three arrays had four activated sites for both stimulation and recording. After placing the electrode arrays, individual recordings were made with stimulation driven through one of the activated electrode arrays while recording neural activity from all 3 arrays. All neural activity was recorded at 30 kHz. During each recording, 1000 ICMS pulses were driven through a single channel on the selected electrode array. ICMS pulses were single-pulse, cathodal-leading biphasic pulses (200 μs/phase, 50 μA) with 200 ms between pulses. The channel with the lowest impedance on each array was chosen for stimulation. After separate recordings were made with stimulation through each array, all three arrays were removed from the cortex, either the somatosensory or premotor

array was moved to a new location, and the arrays were reinserted into cortex. This process was repeated until each combination of sensory and premotor regions was stimulated and recorded. Except for the PM-face, each region with an activated electrode array was stimulated. Stimulation was not performed in the PM-face region to avoid spurious results due to activation of neighboring distal forelimb regions via volume conduction.

Neural Data Processing

Neural recordings were then analyzed to examine ICMS-evoked neural activity. Following the 400 μs stimulus pulse (200 μs/phase), the post-stimulus electrical artifact consisted of a brief period of amplifier saturation with a slow fall-off lasting over 10 ms (Fig 1A). For each channel, this period of saturation was determined quantitatively to set the absolute blanking period from 0.5 ms before the stimulus pulse to 0.25 ms after amplifier saturation ended. Data within this blanking period was set to 0. The remaining portion of the stimulation artifact was removed by using a sliding polynomial fit (32). An 8th order polynomial was fit to the neural data following each stimulus pulse using a 6 ms sliding window. The fit data was then subtracted from the recorded data allowing action potentials to be detected ~1 ms after each stimulus pulse. Periods with artifact were excluded using a nonlinear energy operator and filtered with a single-pole infinite impulse response high-pass filter with a cutoff frequency of 500Hz. Finally, multi-unit action potentials were detected using a threshold detector set at -3.5 x the RMS voltage for each channel (Fig. 1B).

All multi-unit activity was aligned to the stimulus onsets (Fig. 1C). Next, to determine the mesoscale ICMS-evoked firing for a single array, multi-unit spike times were pooled across each channel on an electrode array and the global stimulus-evoked neural activity in the first 25 ms following the stimulus pulse was estimated using a kernel smoothing estimate with a normal

kernel function (Fig. 1D). A reshuffling procedure was used to determine the neural activity expected by chance. Specifically, for each stimulus pulse, a random start time within the inter-stimulus period was chosen. Multi-unit spike times were then aligned to this time point, pooled across channels with data from the beginning of the inter-stimulus period wrapped around to the end, and the chance global firing rate was estimated using a kernel smoothing estimate. This reshuffling procedure was repeated 10,000 times to produce estimates of the chance neural activity. To examine directly connected regions, we considered the transmission time of non-human primate corticocortical connections. Based on estimates of corticocortical conduction velocity (33), and distances between electrode sites used (3-12 mm), we expect conduction delays of ~0.8 ms (range 0.33-3.0 ms) for antidromic potentials with an additional synaptic delay for monosynaptic orthodromic potentials (34, 35). Accounting for these delays, the short-latency stimulus-evoked neural activity was estimated by summing the stimulus-evoked activity in the first 2.5 ms following the stimulus pulse. The statistical significance was determined by indexing the actual short-latency stimulus-evoked neural activity into the reshuffled stimulus-evoked neural activity with a significance threshold of $p<0.05$ with Bonferroni correction for the total number of pairs of regions tested in each monkey. For significant connections, the depth of modulation was calculated by dividing the short-latency stimulus-evoked neural activity by the mean of the reshuffled data.

Comparison with Anatomical Connectivity

Because the experiments described here were followed by an additional imaging experiment (28), it was not possible to use anatomical tracers to directly compare short-latency ICMS-evoked neural activity to anatomical connectivity. Therefore, the ICMS-evoked neural activity was compared to literature-based anatomical connectivity (18-21, 30, 36-41). Studies

using anterograde and retrograde anatomical tracer injections into the sensorimotor system in new world monkeys (owl monkeys, titi monkeys, squirrel monkeys, and capuchin monkeys) were examined to develop a map of sensorimotor connectivity (Fig. 2). Where quantitative estimates of the number of connections were available, a connection between two regions was classified as minor (present with <2% of connections), moderate (2-10%) of connections within a region, or major (>10% of connections within a region). In studies without quantification of the number of connections, we reviewed and qualitatively assigned connections to the 3 categories. The specific connections and sources are summarized in Table 1. Because connections to M1 are heterogeneous with specific connections into rostromedial, rostrolateral, and caudal M1, we subdivided these regions within the map (20, 38, 41). Additionally, because it is uncertain if a unique area 2 is present in squirrel monkeys (31), we pooled reports of area 2 and area 5 connectivity for the region caudal to area 1. In line with reports of anatomical connectivity, all connections were assumed to be reciprocal (18-21).

For each monkey, while electrode insertions were targeted to specific areas, the exact location was dependent upon the pattern of vasculature and extent of the craniectomy. To account for these differences in electrode locations between monkeys, the expected connectivity between electrodes was determined by weighting the sensorimotor connectivity with mixing matrices representing the exact location of each stimulated and recorded electrode array. For stimulation, the current required to activate a region of cortex is proportional to the square of the distance from the stimulating electrode, with estimates of the excitability constant ranging from 100-4000 $\mu A/mm^2$ (13-15). Using our stimulus current of 50 μA the expected directly activated cortical region would have a radius of 0.1-0.7 mm. For this work, the stimulated region was modeled using a border of 0.5 mm around the stimulated electrode array. The connections from

each electrode array were estimated by weighting the connections from each region by the percent of the stimulated area within each region. For the recorded electrode array, the connections to each region were weighted by the percentage of the electrode array within each region. To determine the correspondence between anatomical connectivity and short-latency ICMS-evoked activity, Pearson's r was calculated between the pair-wise anatomical connectivity strengths and the depth-of-modulation of ICMS-evoked activity. The statistical significance of this correspondence was determined by rearranging the areal labels 10,000 times and recalculating the correlation coefficient. The p-value was determined by indexing the actual correlation coefficient into the surrogate distribution of the correlation coefficients.

Stability of ICMS-Evoked Neural Activity

Finally, we sought to determine whether the ICMS-evoked neural activity was stable across the time course of the experiment. Because an electrode was always placed into M1, the premotor-M1 and S1-M1 connections were examined in multiple runs within each monkey. To determine whether the ICMS-evoked neural activity was stable, the correlation (Pearson's r) between the ICMS-evoked neural activity from a single stimulus-recording pair of regions in an individual recording and the ICMS-evoked neural activity from all other pairs of regions from all recordings was calculated. Correlation coefficients were grouped into repeated tests in which the correlation was between ICMS-evoked activity with the same regions tested, and different comparisons in which different pairs of regions were compared. The statistical significance was evaluated using a Wilcoxon's rank-sum test for data from each monkey.

Results

ICMS-Evoked Neural Activity

After removing the stimulus artifact, multi-unit action potentials could be detected on the order of 1 ms post-stimulus with consistent spike waveforms (Fig. 1B). After aligning to the repeated single-pulse ICMS stimuli, as shown in an exemplar channel, clear increases in multi-unit firing could be observed within a few milliseconds (Fig. 1C). When pooled across all channels in an electrode array, the global ICMS-evoked neural activity showed short-latency responses with peaks in neural activity within 2.5 ms post-stimulus (Fig. 1D).

Relationship between ICMS-evoked Neural Activity and Anatomy

In Monkey 1, stimulating/recording electrodes were targeted to areas 1, 3b, 3a and M1, and a recording electrode array was targeted into PMd, PMv, and PM-face. Because of the vascular pattern, the 3a site overlapped the border between areas 3a and 3b and the M1 electrode was placed into rostromedial M1 (Fig. 3A). Figure 3 compares the anatomical connectivity and ICMS-evoked neural activity. Based upon the anatomy, strong connections were expected between M1rm and PMd, and moderate connections were expected between M1rm and PMv. Significant increases in ICMS-evoked neural activity were observed for both pairs or regions with the strongest response in PMd following M1rm stimulation. Across all connections there was a strong correlation between the strength of the expected anatomical connectivity and ICMS-evoked response (Pearson's $r=0.79$, $p=0.0023$).

In Monkey 2, stimulating/recording electrodes were targeted to areas 2/5, 1, 3b, 3a, M1, PMd, PMv, and PM-face. Each region was recorded from and stimulation was performed in all regions except PM-face. Because of the vascular patterns, the area 2/5 electrode overlapped the border with area 1 and the M1 electrode was placed into rostrolateral M1. Additionally, the area stimulated by the electrodes in areas 1 and 3a likely overlapped with area 3b. Figure 4 shows a comparison of the anatomical connections and ICMS-evoked neural activity. Based upon the

anatomy, strong connections were expected between M1rl and PMv, and moderate connections were expected for the M1rl-PMd, M1rl-3a, 3a-PMv, and 2/5/1-PMv connections. Significant increases in ICMS-evoked neural activity were observed for each of these connections except the 2/5/1-PMv connection with the strongest response in PMv following M1rl stimulation. Additionally, ICMS-evoked responses were observed in the PM-face region following stimulation in M1rl and area 2/5/1 but not in response to the other 3 stimulated regions. Across all connections there was a moderately strong correlation between the strength of the expected anatomical connectivity and ICMS-evoked response (Pearson's $r=0.61$, $p=0.0003$).

In Monkey 3, stimulating/recording electrodes were targeted to areas 1, 3b, 3a, M1, PMd, and PMv. Because of the vascular pattern, the M1 electrode was placed into rostromedial M1 and stimulation in area 1 likely activated a small portion of 3b. Figure 5 shows a comparison of the anatomical connectivity and ICMS-evoked neural activity. Based upon the anatomy, moderate to strong connections were expected between M1rm and PMd, PMv, and 3a, and between 3a and both PMd and PMv. Significant increases in ICMS-evoked neural activity were observed for each of these connections with the strongest response for the bidirectional M1rm-PMd and M1rm-PMv connections. Across all connections there was a strong correlation between the strength of the expected anatomical connectivity and ICMS-evoked response (Pearson's $r=0.87$, $p<0.0001$).

Taken together, the known anatomical connections strongly correlated with ICMS-evoked neural activity in each monkey. Figure 6 shows a confusion matrix comparing the strength of anatomical connections to the strength of ICMS-evoked activity across monkeys. The correspondence is driven by the separability of regions with moderate-major anatomical connections and regions with no known anatomical connections. All of the major connections

demonstrated moderate or major modulation of neural activity following ICMS, and 16 of 17 connections with moderate anatomical connectivity showed statistically significant ICMS-evoked increases in neural activity. Finally, 7 of 9 connections with no anatomical connections showed an absence of ICMS-evoked neural activity.

Stability of ICMS-Evoked Responses

Because the PM and S1 electrodes were moved sequentially, connections between M1 and both PM and S1 regions were examined 2-4 times in each monkey. These repeated experimental conditions were used to test the stability of ICMS-evoked neural activity. Figure 7A shows exemplar patterns of ICMS-evoked neural activity for each repetition of two pairs of sites. The amplitude and time course of ICMS-evoked neural firing is maintained across recordings. Across all pairs of regions in each monkey, the correlation between ICMS-evoked neural activity from different recordings was higher for repeated electrode sites than different sites (Fig 7B) (Monkey 1: $p<0.0001$; Monkey 2: $p<0.0001$; Monkey 3: $p=0.0004$).

Discussion

These results show that the observed strength of ICMS-evoked neural activity is significantly correlated to previously described anatomical connectivity. This effect was driven primarily by the presence of ICMS-evoked neural activity between regions with major and moderate anatomical connections. There was more variability in the regions with sparse anatomical connections. Because of the sparser nature of the anatomical connectivity between these regions, it is likely that the placement of any specific electrode location has a greater impact on the pattern of ICMS-evoked activity. Despite this potential limitation, short-latency ICMS-evoked neural activity appears to be a good surrogate for effective anatomical connectivity.

The specific mechanisms that are demonstrated by ICMS-evoked neural activity are an important consideration when comparing it to anatomical connectivity. Because the volume of axons activated and the density of soma activated increases monotonically with stimulus intensity, it is thought that the dominant mode of ICMS is likely activation of axons (12). However, low amplitude stimulation can also lead to transsynaptic activation (16). Therefore, by considering the neural activity <2.5 ms after each ICMS pulse, a combination of antidromic potentials and monosynaptic orthodromic action potentials were likely measured. Because anatomic connectivity between the regions studied is reciprocal (18-21), it is unlikely that the results were impacted by the mixture of antidromic and orthodromic responses.

When pairs of regions were examined multiple times, ICMS-evoked neural activity was stable over the duration of the experiment, despite slight shifts in electrode positions. Therefore, this measure is invariant to slight changes in anesthetic state and minor changes in the specific neural population sampled. While these results do not directly address the stability of ICMS-evoked connectivity over long periods, their within-session repeatability is a minimum criterion for chronic monitoring and assessment. There are likely several important considerations that may impact the transition from acute to chronic electrode arrays. First, these experiments were done under ketamine anesthesia, which potentially disrupts baseline corticocortical information transfer (42), therefore increased background levels of shared corticocortical neural activity in awake animals may limit ICMS-evoked activity between weakly connected regions. Second, the acute arrays used here sampled neural activity at multiple sites within each cortical column. Chronic arrays could sample from a wider spatial region, leading to less dependence on the specific neural population sampled, however it is uncertain if there is a layer-specific distribution of ICMS-evoked responses. Finally, the encapsulation of chronic electrodes by scar tissue could

impact the ability to drive stimulation, however as ICMS thresholds for sensory perception decrease over time (5), it is unlikely that the ability to drive single-pulse ICMS responses would be affected.

Several other methods have also been proposed to examine corticocortical connectivity. In particular, ICMS has also been used in conjunction with fMRI or intrinsic optical imaging to measure intra- and interregional connectivity (22-26, 43). However, the stimulation amplitudes in these studies were several times higher than the amplitudes used here, increasing the risk of cortical damage with repeated stimulation (44). Additionally, while an area of cortex can be repeatably imaged, fMRI in animal models requires the use of anesthesia for scanning and it is technically challenging to maintain the visual field necessary for repeated optical imaging . Finally, because these measures capture the hemodynamic response, it is uncertain whether they represent subthreshold synaptic potentials or action potentials (26). In contrast, with a chronic electrode array, it would be easy to adapt our methodology for examining ICMS-evoked neural activity to longitudinal measurements in awake animals. While the horizontal of spread of neural activity has previously been examined within a single electrode array (45), this is the first report of the correspondence between mesoscale anatomical and evoked connectivity using ICMS-evoked neural activity.

The ability to perform longitudinal experiments using chronic arrays is particularly significant for studies examining recovery from neural injuries. Following a stroke, neuroplasticity leads to changes in connectivity within and between unaffected cortical regions. Within the motor system, these alterations can be seen in changes in motor map outputs (7, 9), alterations in patterns of functional connectivity (46-49), and alterations in anatomical connections (50). Because specific changes in map output and connectivity have been observed

after functional recovery (7, 9), it is thought that these changes are associated with functional recovery. However, as the time course of motor map reorganization is distinct from the time course of behavioral recovery (8), the specific relationship between changes in anatomical and functional connectivity remains uncertain. Because causal relationships must demonstrate temporal precedence, determining the specific relevance of changes in corticocortical connectivity with respect to behavioral changes will require assessing changes in connectivity with high temporal specificity.

There are also several limitations to note. Because the animals were used for a subsequent experiment, we were unable to compare ICMS-evoked activity to anatomical connections within the same animals. However, the literature-based estimates of anatomical connections, combined with cortical mapping to determine specific electrode locations, likely produced accurate estimates of anatomical connectivity between sites. Second, the experiments used acute electrode arrays that were repeatedly reinserted and could possibly damage the cortex. However, the stability of ICMS-evoked neural activity shows that damage to neural populations did not significantly impact the results. Finally, the stimulation paradigm used single-pulse ICMS delivered at set 200 ms intervals. This constant interstimulus interval could lead to some entrainment of neural activity (51). However, changes in neuronal excitability and entrainment should impact the reshuffled control data in addition to the ICMS-evoked response. Therefore, it is unlikely that the set stimulus timing impacted the results presented.

Conclusion

We have demonstrated that neural activity evoked from ICMS in a nearby region can be used to examine mesoscale corticocortical connectivity. This will be especially valuable for examining longitudinal changes in corticocortical connectivity associated with a brain injury,

neural disorder, or therapeutic. Future studies will extend these analyses to chronic experiments in healthy animals and animals recovering from cortical lesions.

Declaration of competing interests

The authors have no conflicts of interest related to the current work to report.

Funding

This work was supported by the National Institutes of Health (www.nih.gov: NIH Grants R01NS030853 and R01NS118918) and the Landon Center on Aging.

Tables

Table 1: Literature-reported anatomical connection strengths

Target Region	Connection Region	Connection Strength	Species	References
M1	PMv	+++	Squirrel Monkey, Owl Monkey, Cebus Monkey	(18-20, 37, 41)
	PMd	+++	Squirrel Monkey, Owl Monkey, Cebus Monkey	(19, 20, 37)
	3a	++/+++	Squirrel Monkeys, Owl Monkeys	(20, 37)
	3b	+/++	Squirrel Monkeys, Owl Monkey	(20, 37)
	1	++	Squirrel Monkeys, Owl Monkey	(20, 37)
	2	++	Owl Monkey	(20)
PMv	M1rl	+++	Squirrel Monkey, Owl Monkey, Cebus Monkey	(18, 19, 21, 37, 38, 41)
	3a	+/++	Squirrel Monkey, Owl Monkey	(18, 21, 37)
	3b	+	Squirrel Monkey, Owl Monkey	(18, 21, 37)
	1	+/++	Squirrel Monkey, Owl Monkeys	(18, 21, 37)
	2	++	Owl Monkey	(21)
PMd	M1rm	+++	Squirrel Monkey, Owl Monkey, Cebus Monkey	(19, 21, 37, 38)
	3a	-/++	Squirrel Monkey, Owl Monkey	(21, 37)
	3b	-/+	Squirrel Monkey, Owl Monkey	(21, 37)
	1	+	Squirrel Monkey, Owl Monkey	(21, 37)
	2	+	Owl Monkey	(21)
3a	PMv	+	Squirrel Monkey	(18)
3b	M1c	+/++	Squirrel Monkey, Titi Monkey	(30, 39, 40)
	PMv	+	Squirrel Monkey	(18)
	PMd	+	Squirrel Monkey	(39)
1	M1c	++	Squirrel Monkey, Titi Monkey	(30, 36)
	PMv	+	Squirrel Monkey, Titi Monkey	(30, 36)
	PMd	+	Squirrel Monkey, Titi Monkey	(30, 36)
1/2	PMv	+	Squirrel Monkey	(18)
2/5	M1	++	Titi Monkey	(30)
	PMv	++	Titi Monkey	(30)
	PMd	++	Titi Monkey	(30)

Connection Strength: +++ Major Connection, ++ Moderate Connection, + Minor Connection, - Absent Connection

Figures

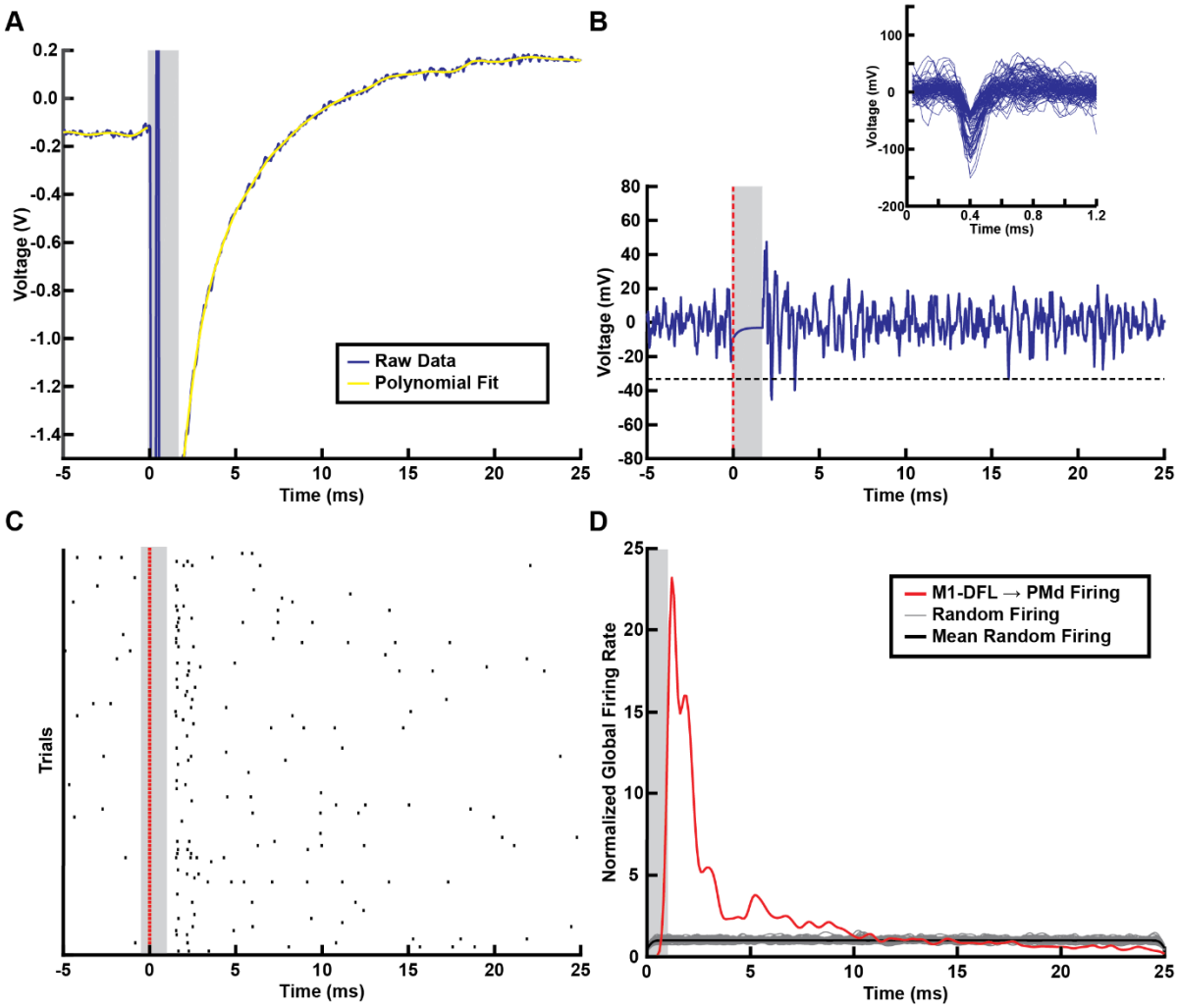

Figure 1: Stimulus artifact correction. A. Single-pulse ICMS stimulation produced an initial large amplitude artifact that with a slow return to baseline. The unusable period of the data (~1 ms post-stimulus) in which the stimulation was ongoing, or the amplifiers were saturated was automatically detected and set to zero. A sliding polynomial fit was used to detect the remaining stimulus artifact (yellow) and the stimulus was subtracted from the data. **B.** Following artifact removal multi-unit action potentials were detected using a threshold detector (black line). Action potentials with characteristic spike profiles (inset) could be detected as early as 1 ms post-stimulation (red line). **C.** An exemplar channel shows a clear increase in multi-unit spikes 1-2 ms post-stimulus. **D.** To capture mesoscale connectivity the neural response in all electrodes within an array were pooled to reveal the global ICMS-evoked neural activity between sensorimotor regions (red trace). The significance of responses was assessed by randomly altering the temporal relationship between the ICMS pulse and neural activity across 1000 individual ICMS

pulses (gray traces). In the exemplar shown, stimulation in the M1 distal forelimb region produced a strong short latency (<2.5 ms) increase in neural activity within PMd.

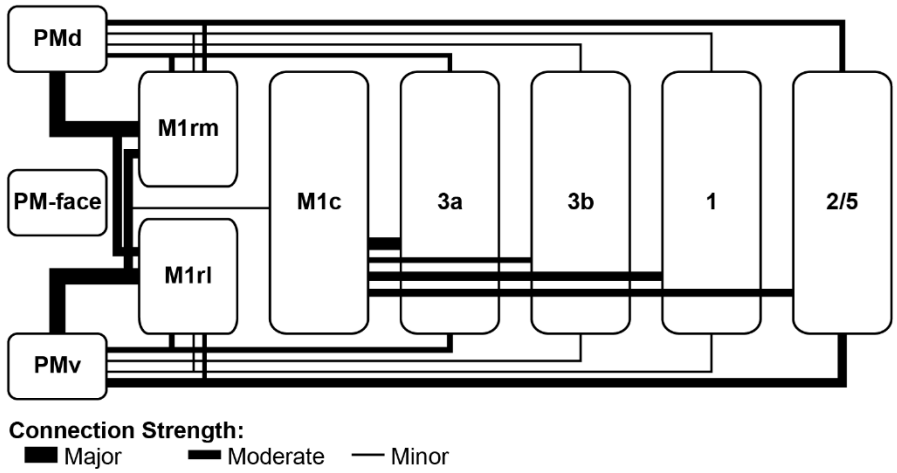

Figure 2: Anatomical connectivity map. The expected anatomical connectivity between sensorimotor regions of the squirrel monkey was compiled from prior literature sources using anatomical tracers to assess connectivity in new world non-human primate species.

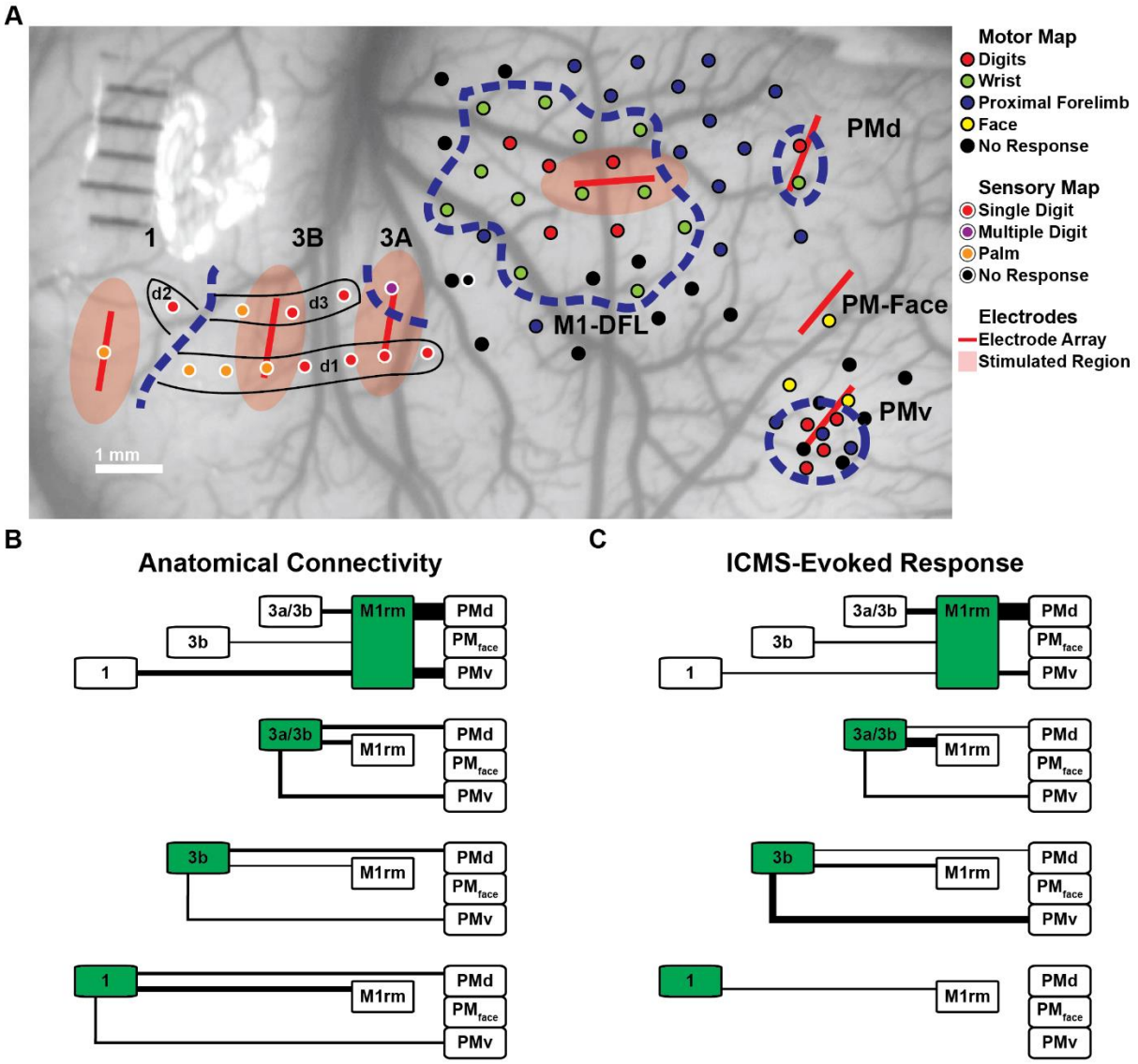

Figure 3: Comparison between anatomical and ICMS-evoked connectivity (Monkey 1). A. In Monkey 1 stimulating/recording electrodes were placed in the rostromedial portion of the M1 distal forelimb region, across the area 3a/3b border, in area 3b, and area 1, and recording electrodes were placed in PMd, PMV, and the face region of M1 in between PMD and PMv. Motor regions were assessed using ICMS mapping (black-outlined sites), and sensory region boundaries were assessed using sensory mapping (white-outlined sites). Electrodes (red lines) were targeted to single brain regions, but the specific placement was adjusted to fit the vasculature pattern. Red shadings show the regions expected to be activated by the 50 µA ICMS pulse **B.** Expected anatomical connectivity was assessed by weighting the literature-based anatomical connectivity map by the portion of each anatomical region expected to be stimulated and recorded from using the specific electrode locations and regional boundaries (**A**). Line thicknesses represent the normalized number of anatomical connections **C.** Short-latency ICMS-

evoked neural activity was evaluated for each connection. Regions highlighted in green represent stimulated areas and the line thicknesses show the depth-of-modulation of ICMS-evoked increases in neural activity. The ICMS-evoked activity was significantly correlated to the expected anatomical connectivity ($r=0.79$, $p=0.0023$), with the strongest connectivity observed between M1rm and PMd.

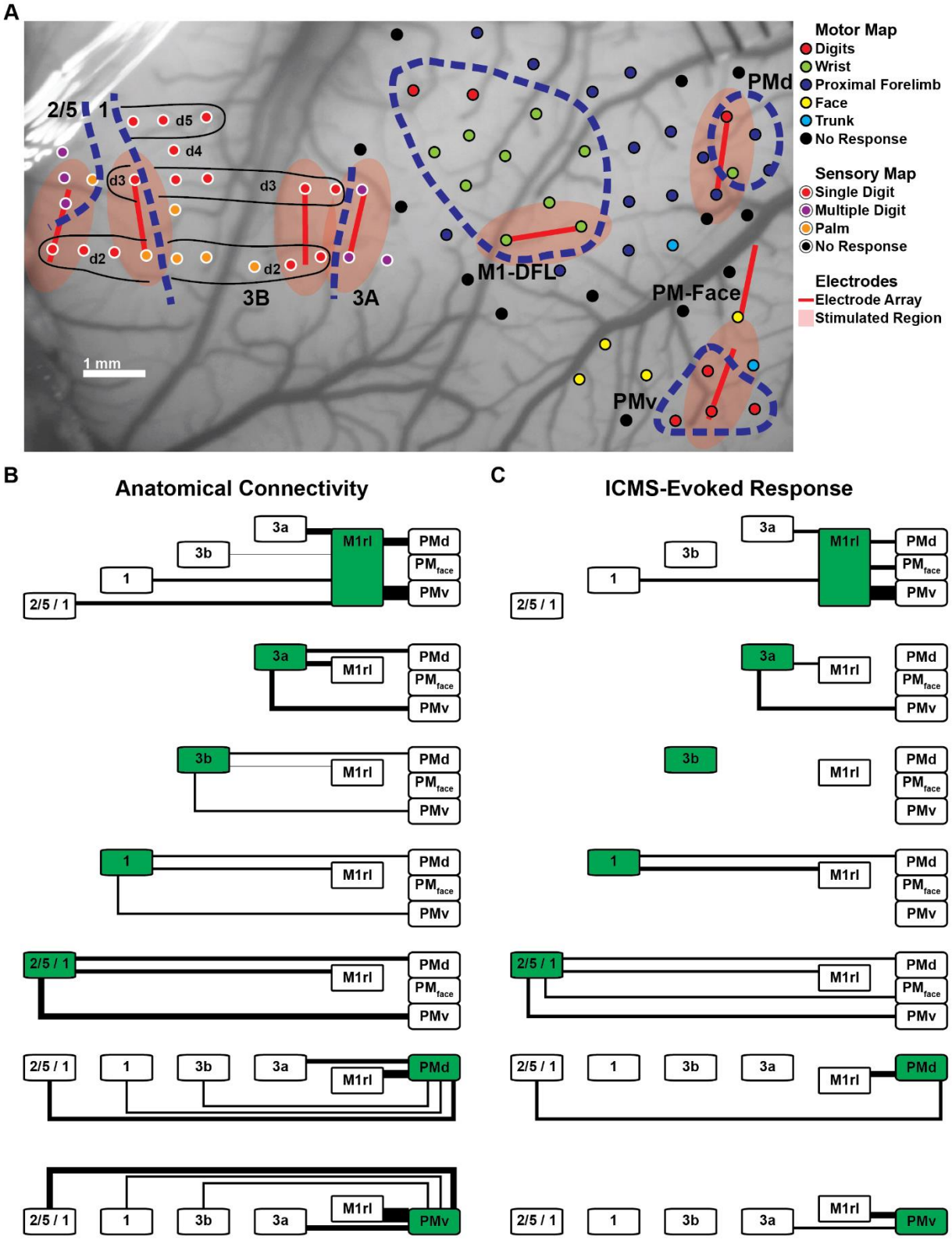

Figure 4: Comparison between anatomical and ICMS-evoked connectivity (Monkey 2). A. In Monkey 2 stimulating/recording electrodes were placed in the rostrolateral portion of the M1

distal forelimb region, in PMv, PMd, the face region of premotor cortex, area 3a, area 3b, area 1, and across the border between area 1 and area 2/5. All regions were stimulated except for PM-face. The specific placement of electrodes (red lines) was adjusted to fit the vasculature pattern. Red shadings show the area expected to be activated by the 50 µA ICMS pulse **B.** Expected anatomical connectivity was assessed by weighting the literature-based anatomical connectivity by the portion of specific regions stimulated and recorded from (**A**). Line thicknesses represent the expected number of anatomical connections **C.** Short latency ICMS-evoked neural activity was evaluated for each connection. Regions highlighted in green represent stimulated areas and the line thicknesses show the depth-of-modulation of ICMS-evoked increases in neural activity. The ICMS-evoked activity was significantly correlated to the expected anatomical connectivity ($r=0.61$, $p=0.0003$), with the strongest connectivity observed between M1rl and PMv.

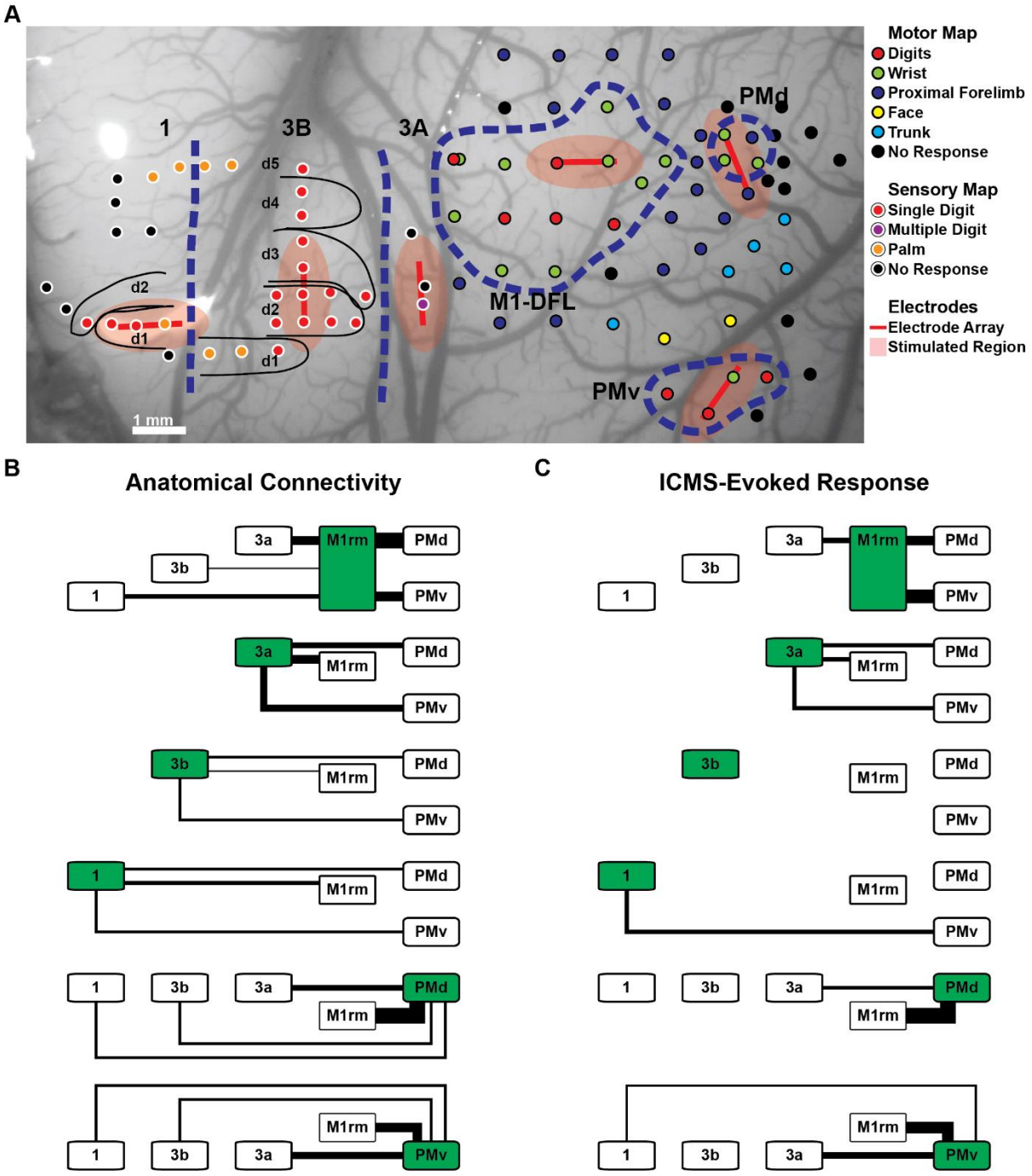

Figure 5: Comparison between anatomical and ICMS-evoked connectivity (Monkey 3). A. In Monkey 3 stimulating/recording electrodes were placed in the rostromedial portion of the M1 distal forelimb region, PMv, PMd, area 3a, area 3b, and area 1. Motor regions were assessed using ICMS mapping (black-outlined sites), and sensory region boundaries were assessed using sensory mapping (white-outlined sites). The specific electrode placement was adjusted to fit the vasculature pattern. Red shadings show the regions expected to be activated by the 50 µA ICMS

pulse **B.** Expected anatomical connectivity was assessed by weighting the literature-based anatomical connectivity by the portion of each region stimulated and recorded from. Line thicknesses represent the expected number of anatomical connections **C.** Short latency ICMS-evoked neural activity was evaluated for each connection. Regions highlighted in green represent stimulated areas and the line thicknesses show the depth-of-modulation of ICMS-evoked increases in neural activity. The ICMS-evoked activity was significantly correlated to the expected anatomical connectivity ($r=0.87$, $p<0.0001$), with significant ICMS-evoked neural activity in the regions expected to have moderate-strong anatomical connectivity (3a, M1, PMd, and PMv).

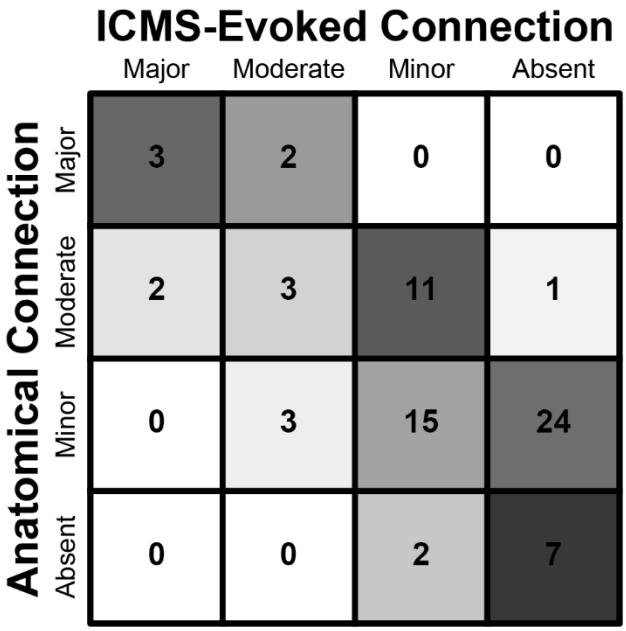

Figure 6: Anatomical and ICMS-evoked connectivity confusion matrix. The strength of anatomical and ICMS-evoked activity was linearly discretized and compared. Across monkeys, the ICMS-evoked activity correlated with anatomical connectivity. This effect was driven by the presence of significant ICMS-evoked neural activity when moderate-major anatomical connectivity is present, and an absence of ICMS-evoked neural activity when no anatomical connectivity has been reported. Shadings are normalized to the total number of connections in each category of anatomical connectivity.

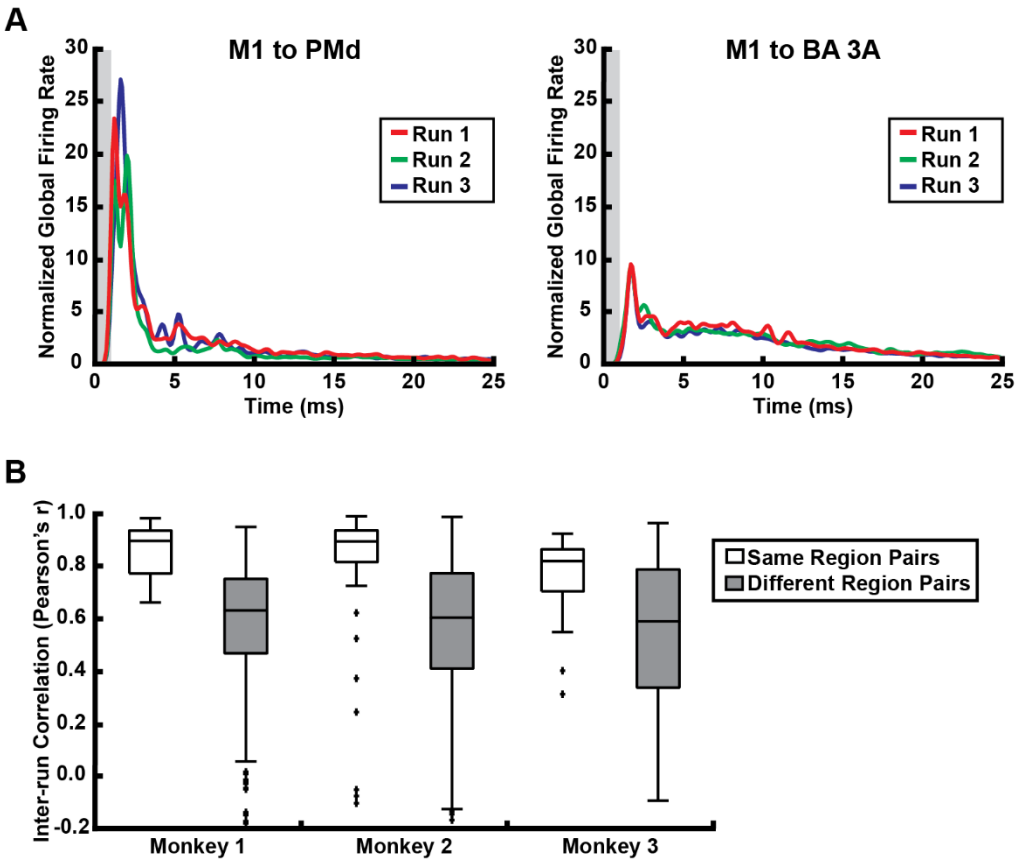

Figure 7: Stability of ICMS-evoked neural responses. To examine the stability of ICMS-evoked neural activity, connections that were evaluated in multiple recordings were examined. **A.** Exemplar responses are shown from Monkey 1 in PMd (left) and area 3a (right) after M1 stimulation. Each area shows a clear and distinct stimulus-evoked increase in neural activity that is maintained across recordings. **B.** The stability across connections was evaluated by comparing the correlations of ICMS-evoked neural activity between pairs of recordings with repeated electrode positions to the correlations of ICMS-evoked neural activity between pairs of recordings with different electrode positions. The ICMS responses for repeated electrode locations were significantly more correlated than for different locations, showing the ICMS-evoked neural responses were stable over the course of the experiment in each monkey.

References

1. Antal A, Boros K, Poreisz C, Chaieb L, Terney D, Paulus W. Comparatively weak after-effects of transcranial alternating current stimulation (tACS) on cortical excitability in humans. Brain Stimul. 2008;1(2):97-105.
2. Tik M, Hoffmann A, Sladky R, Tomova L, Hummer A, Navarro de Lara L, et al. Towards understanding rTMS mechanism of action: Stimulation of the DLPFC causes network-specific increase in functional connectivity. Neuroimage. 2017;162:289-96.
3. Ritaccio AL, Brunner P, Schalk G. Electrical Stimulation Mapping of the Brain: Basic Principles and Emerging Alternatives. J Clin Neurophysiol. 2018;35(2):86-97.
4. Allison-Walker T, Hagan MA, Price NSC, Wong YT. Microstimulation-evoked neural responses in visual cortex are depth dependent. Brain Stimul. 2021;14(4):741-50.
5. Hughes CL, Flesher SN, Weiss JM, Downey JE, Boninger M, Collinger JL, et al. Neural stimulation and recording performance in human sensorimotor cortex over 1500 days. J Neural Eng. 2021;18(4).
6. Salzman CD, Murasugi CM, Britten KH, Newsome WT. Microstimulation in visual area MT: effects on direction discrimination performance. J Neurosci. 1992;12(6):2331-55.
7. Frost SB, Barbay S, Friel KM, Plautz EJ, Nudo RJ. Reorganization of remote cortical regions after ischemic brain injury: a potential substrate for stroke recovery. J Neurophysiol. 2003;89(6):3205-14.
8. Nishibe M, Urban ET, 3rd, Barbay S, Nudo RJ. Rehabilitative training promotes rapid motor recovery but delayed motor map reorganization in a rat cortical ischemic infarct model. Neurorehabil Neural Repair. 2015;29(5):472-82.
9. Nudo RJ, Milliken GW. Reorganization of movement representations in primary motor cortex following focal ischemic infarcts in adult squirrel monkeys. J Neurophysiol. 1996;75(5):2144-9.
10. Nudo RJ, Milliken GW, Jenkins WM, Merzenich MM. Use-dependent alterations of movement representations in primary motor cortex of adult squirrel monkeys. J Neurosci. 1996;16(2):785-807.
11. Nudo RJ, Wise BM, SiFuentes F, Milliken GW. Neural substrates for the effects of rehabilitative training on motor recovery after ischemic infarct. Science. 1996;272(5269):1791-4.
12. Kumaravelu K, Sombeck J, Miller LE, Bensmaia SJ, Grill WM. Stoney vs. Histed: Quantifying the spatial effects of intracortical microstimulation. Brain Stimul. 2022;15(1):141-51.
13. Stoney SD, Jr., Thompson WD, Asanuma H. Excitation of pyramidal tract cells by intracortical microstimulation: effective extent of stimulating current. J Neurophysiol. 1968;31(5):659-69.
14. Tehovnik EJ. Electrical stimulation of neural tissue to evoke behavioral responses. J Neurosci Methods. 1996;65(1):1-17.
15. Tehovnik EJ, Tolias AS, Sultan F, Slocum WM, Logothetis NK. Direct and indirect activation of cortical neurons by electrical microstimulation. J Neurophysiol. 2006;96(2):512-21.
16. Asanuma H, Rosen I. Spread of mono- and polysynaptic connections within cat's motor cortex. Exp Brain Res. 1973;16(5):507-20.
17. Shanks MF, Pearson RC, Powell TP. The ipsilateral cortico-cortical connexions between the cytoarchitectonic subdivisions of the primary somatic sensory cortex in the monkey. Brain Res. 1985;356(1):67-88.

18. Dancause N, Barbay S, Frost SB, Plautz EJ, Stowe AM, Friel KM, et al. Ipsilateral connections of the ventral premotor cortex in a new world primate. J Comp Neurol. 2006;495(4):374-90.
19. Dum RP, Strick PL. Frontal lobe inputs to the digit representations of the motor areas on the lateral surface of the hemisphere. J Neurosci. 2005;25(6):1375-86.
20. Stepniewska I, Preuss TM, Kaas JH. Architectonics, somatotopic organization, and ipsilateral cortical connections of the primary motor area (M1) of owl monkeys. J Comp Neurol. 1993;330(2):238-71.
21. Stepniewska I, Preuss TM, Kaas JH. Ipsilateral cortical connections of dorsal and ventral premotor areas in New World owl monkeys. J Comp Neurol. 2006;495(6):691-708.
22. Card NS, Gharbawie OA. Principles of Intrinsic Motor Cortex Connectivity in Primates. J Neurosci. 2020;40(22):4348-62.
23. Friedman RM, Morone KA, Gharbawie OA, Roe AW. Mapping mesoscale cortical connectivity in monkey sensorimotor cortex with optical imaging and microstimulation. J Comp Neurol. 2020;528(17):3095-107.
24. Sawaguchi T. Modular activation and suppression of neocortical activity in the monkey revealed by optical imaging. Neuroreport. 1994;6(1):185-9.
25. Stepniewska I, Friedman RM, Gharbawie OA, Cerkevich CM, Roe AW, Kaas JH. Optical imaging in galagos reveals parietal-frontal circuits underlying motor behavior. Proc Natl Acad Sci U S A. 2011;108(37):E725-32.
26. Tolias AS, Sultan F, Augath M, Oeltermann A, Tehovnik EJ, Schiller PH, et al. Mapping cortical activity elicited with electrical microstimulation using FMRI in the macaque. Neuron. 2005;48(6):901-11.
27. Council NR. Guide for the Care and Use of Laboratory Animals: Eighth Edition. Washington, DC: The National Academies Press; 2011. 246 p.
28. Chang KW, Zhu Y, Hudson HM, Barbay S, Guggenmos DJ, Nudo RJ, et al. Photoacoustic imaging of squirrel monkey cortical and subcortical brain regions during peripheral electrical stimulation. Photoacoustics. 2022;25:100326.
29. Sur M, Nelson RJ, Kaas JH. Representations of the body surface in cortical areas 3b and 1 of squirrel monkeys: comparisons with other primates. J Comp Neurol. 1982;211(2):177-92.
30. Padberg J, Disbrow E, Krubitzer L. The organization and connections of anterior and posterior parietal cortex in titi monkeys: do New World monkeys have an area 2? Cereb Cortex. 2005;15(12):1938-63.
31. Padberg J, Franca JG, Cooke DF, Soares JG, Rosa MG, Fiorani M, Jr., et al. Parallel evolution of cortical areas involved in skilled hand use. J Neurosci. 2007;27(38):10106-15.
32. Wagenaar DA, Potter SM. Real-time multi-channel stimulus artifact suppression by local curve fitting. J Neurosci Methods. 2002;120(2):113-20.
33. Ferraina S, Pare M, Wurtz RH. Comparison of cortico-cortical and cortico-collicular signals for the generation of saccadic eye movements. J Neurophysiol. 2002;87(2):845-58.
34. Katz B, Miledi R. The Measurement of Synaptic Delay, and the Time Course of Acetylcholine Release at the Neuromuscular Junction. Proc R Soc Lond B Biol Sci. 1965;161:483-95.
35. Lin JW, Faber DS. Modulation of synaptic delay during synaptic plasticity. Trends Neurosci. 2002;25(9):449-55.
36. Cerkevich CM, Kaas JH. Corticocortical projections to area 1 in squirrel monkeys (Saimiri sciureus). Eur J Neurosci. 2019;49(8):1024-40.

37. Gharbawie OA, Stepniewska I, Kaas JH. Cortical connections of functional zones in posterior parietal cortex and frontal cortex motor regions in new world monkeys. Cereb Cortex. 2011;21(9):1981-2002.
38. Hamadjida A, Dea M, Deffeyes J, Quessy S, Dancause N. Parallel Cortical Networks Formed by Modular Organization of Primary Motor Cortex Outputs. Curr Biol. 2016;26(13):1737-43.
39. Liao CC, Gharbawie OA, Qi H, Kaas JH. Cortical connections to single digit representations in area 3b of somatosensory cortex in squirrel monkeys and prosimian galagos. J Comp Neurol. 2013;521(16):3768-90.
40. Negyessy L, Palfi E, Ashaber M, Palmer C, Jakli B, Friedman RM, et al. Intrinsic horizontal connections process global tactile features in the primary somatosensory cortex: neuroanatomical evidence. J Comp Neurol. 2013;521(12):2798-817.
41. Dancause N, Barbay S, Frost SB, Plautz EJ, Popescu M, Dixon PM, et al. Topographically divergent and convergent connectivity between premotor and primary motor cortex. Cereb Cortex. 2006;16(8):1057-68.
42. Schroeder KE, Irwin ZT, Gaidica M, Nicole Bentley J, Patil PG, Mashour GA, et al. Disruption of corticocortical information transfer during ketamine anesthesia in the primate brain. Neuroimage. 2016;134:459-65.
43. Brock AA, Friedman RM, Fan RH, Roe AW. Optical imaging of cortical networks via intracortical microstimulation. J Neurophysiol. 2013;110(11):2670-8.
44. McCreery D, Han M, Pikov V, Miller C. Configuring intracortical microelectrode arrays and stimulus parameters to minimize neuron loss during prolonged intracortical electrical stimulation. Brain Stimul. 2021;14(6):1553-62.
45. Hao Y, Riehle A, Brochier TG. Mapping Horizontal Spread of Activity in Monkey Motor Cortex Using Single Pulse Microstimulation. Front Neural Circuits. 2016;10:104.
46. Bauer AQ, Kraft AW, Wright PW, Snyder AZ, Lee JM, Culver JP. Optical imaging of disrupted functional connectivity following ischemic stroke in mice. Neuroimage. 2014;99:388-401.
47. Blaschke SJ, Hensel L, Minassian A, Vlachakis S, Tscherpel C, Vay SU, et al. Translating Functional Connectivity After Stroke: Functional Magnetic Resonance Imaging Detects Comparable Network Changes in Mice and Humans. Stroke. 2021;52(9):2948-60.
48. Carter AR, Patel KR, Astafiev SV, Snyder AZ, Rengachary J, Strube MJ, et al. Upstream dysfunction of somatomotor functional connectivity after corticospinal damage in stroke. Neurorehabil Neural Repair. 2012;26(1):7-19.
49. van Meer MP, van der Marel K, Wang K, Otte WM, El Bouazati S, Roeling TA, et al. Recovery of sensorimotor function after experimental stroke correlates with restoration of resting-state interhemispheric functional connectivity. J Neurosci. 2010;30(11):3964-72.
50. Dancause N, Barbay S, Frost SB, Plautz EJ, Chen D, Zoubina EV, et al. Extensive cortical rewiring after brain injury. J Neurosci. 2005;25(44):10167-79.
51. Butovas S, Schwarz C. Spatiotemporal effects of microstimulation in rat neocortex: a parametric study using multielectrode recordings. J Neurophysiol. 2003;90(5):3024-39.